A Pore-Scale Investigation of Low salinity water flooding in Porous Media: Uniformly Wetted Systems

A Pore-Scale Investigation of Low-Salinity Waterflooding in Porous Media: Uniformly Wetted Systems

Michael G. Watson[a,*], Igor Bondino[c], Gerald Hamon[c] and Steven R. McDougall[b]

[a]*School of Mathematics & Statistics, University of Sydney, NSW 2006, Australia*
[b]*Institute of Petroleum Engineering, Heriot-Watt University, Edinburgh, EH14 4AS, Scotland*
[c]*Total E&P, Avenue Larribau, 64018, Pau, France*
**Corresponding Author: Tel.: +61293514077; E-mail: michael.watson@sydney.edu.au*

Abstract

The potential of low-salinity (LS) water injection as an oil recovery technique has been the source of much recent debate within the petroleum industry. Evidence from both laboratory and field-level studies has indicated significant benefits compared to conventional high-salinity (HS) waterflooding, but many conflicting results have also been reported and, to date, the underlying mechanisms remain poorly understood. In this paper, we aim to address this uncertainty by developing a novel, steady-state pore network model in which LS brine displaces oil from a HS-bearing network. The model allows systematic investigation of the crude oil/brine/rock parameter space, with the goal of identifying features that may be critical to the production of incremental oil following LS brine injection. By coupling the displacement model to a salinity-tracking tracer algorithm, and assuming that a reduction of water salinity within the pore network leads to localised wettability alteration, substantial perturbations to standard pore filling sequences are predicted. The results clearly point to two principal effects of dynamic contact angle modification at the pore-scale: a "pore sequence" effect, characterised by an alteration to the distribution of displaced pore sizes; and a "sweep efficiency" effect, demonstrated by a change in the overall fraction of pores invaded. Our study indicates that any LS effect will depend on the relative (scenario-dependent) influence of each mechanism, where factors such as the initial wettability state of the system and the pore size distribution of the underlying network are found to play crucial roles. In addition, we highlight the important role played by end-point capillary pressure in determining LS efficacy.

Keywords

Pore network modelling
Two-phase flow
Low-salinity waterflooding
Wettability modification
Enhanced oil recovery

Acknowledgements

The authors would like to thank Total E&P for their financial support, technical assistance and permission to publish the paper.

1. Introduction

Historically, the reservoir engineering practice of waterflooding was widely utilised as a mechanism for reservoir pressure maintenance; however, in many cases it is now applied as a recovery technique at the very beginning of oil field development. A breadth of recent experimental evidence has suggested that oil recovery is strongly influenced by the composition of both the injected and connate brines, with significant effort focussed towards the apparent potential of low-salinity (LS) water to increase oil production in both secondary and tertiary modes.

The earliest reported observations of this effect can be attributed to Martin (1959) and Bernard (1967), both of whom presented results indicating that injection of fresh water, rather than high-salinity (HS) brine, improved the recovery of oil from sandstone cores. While this early research did not receive much attention from the petroleum industry, interest in the topic has gathered pace over recent years – largely driven by the work of Morrow and colleagues (Jadhunandan and Morrow 1995; Yildiz and Morrow 1996; Tang and Morrow 1997; Morrow et al. 1998; Tang and Morrow 1999a; Tang and Morrow 1999b). These early laboratory studies began to identify conditions deemed to be necessary for improved oil recovery by LS injection in sandstones – significant clay content in the core, the presence of connate water and exposure to crude oil, for example – but, to date, the precise mechanisms underlying this "low-salinity effect" (LSE) remain poorly understood. Although most published experimental LS data relates to waterflooding in sandstone rocks, recent evidence has indicated that the phenomenon of improved recovery by LS injection may also exist in carbonates (Yousef et al. 2010).

A number of potential LS mechanisms have been proposed in the literature, such as: fines migration (Tang and Morrow 1999b), alkaline flooding (McGuire et al. 2005), multi-component ionic exchange (Lager et al. 2006), electrical double layer expansion (Ligthelm et al. 2009; Mahani et al. 2015) and pH-driven wettability alteration (Austad et al. 2010). Unfortunately, despite extensive research in this regard, a single widely accepted candidate has yet to emerge; indeed, the existence of contradictory results in many cases strongly suggests that more than one mechanism may be at play. Importantly, the overall consequence of many of the suggested mechanisms is believed to be (either directly or indirectly) an alteration of the underlying wettability state of the crude oil/brine/rock (COBR) system. In the most general terms, this LS-induced wettability alteration – which is frequently deemed to be towards increased water-wetness – can be interpreted as a disturbance of the established chemical equilibrium that may alter the rock surface properties by processes such as adsorption, desorption and dissolution. The recent review papers by Morrow and Buckley (2011) and Skauge (2013) present a comprehensive discussion of the current low-salinity waterflooding (LSW) literature and further details of the various proposed mechanisms.

While there remains no clear understanding of why LSW might lead to improved oil recovery, it appears likely that the process involves a complex interplay among a number of controlling parameters. Inevitably, this makes it extremely difficult to design suitable laboratory experiments where individual factors can be studied in isolation. A favourable alternative, therefore, is the use of network modelling techniques – an approach that enables the pore-scale displacement behaviour to be analysed in a controlled manner with regard to pertinent parameters, such as rock structure, fluid composition and system wettability.

Pore network models have been widely applied in the oil industry to study two- and three-phase fluid displacements in a variety of contexts (McDougall and Sorbie 1997; Blunt 2001; Mahmud et al. 2007). The methodology proposed in this paper represents, to our knowledge, the first attempt to simulate LSW and associated wettability modification at the pore-scale. While the assumptions underlying this approach are similar to those proposed in the theoretical model of Sorbie and Collins (2010), the current study is more wide-ranging and, importantly, allows investigation of the influence of spatial effects, which were absent in their analysis. By coupling a steady-state oil displacement model to a brine salinity-tracking tracer algorithm, we examine the impact of dynamic wettability alteration on pore-level filling sequences and perform a comprehensive sensitivity study to identify parameters that may be critical to the production of additional oil following LS injection in networks of uniform wettability. The full modelling rationale is described in detail below, followed by the presentation and discussion of a broad range of simulation results, before appropriate conclusions are drawn.

2. Model Description

Although the experimental core-flooding literature highlights a number of inconsistencies between LS studies, it is clear that the injection of LS brine as a recovery technique is likely to involve complex geo-chemical interactions with the connate brine, crude oil and the mineral substrate. Whilst the precise response will depend strongly upon the particular fluid compositions and rock mineralogy under consideration, it is generally understood that the introduction of LS brine leads to an alteration in system wettability. Therefore, in order to limit the complexity of the pore network modelling approach that we implement here, explicit chemical effects are neglected, and we focus instead on the pore-level *consequences* of the underlying chemistry through its dynamic modification of rock wettability. Using this approach, it is possible to study the impact of a wide variety of COBR parameters that may be critical in determining the existence and extent of any LSE.

The parameter space to be investigated is sizeable and many simulations are required to allow general conclusions to be drawn. Hence, rather than utilising a computationally-intensive fully unsteady-state displacement model at this stage, we choose to adapt a steady-state approach by making a number of reasonable assumptions that allow us to estimate the *dynamic* evolution of the aqueous phase within the network. This is achieved by coupling the steady-state displacement model with a tracer injection algorithm that tracks the spatio-temporal progression of water salinity as the injected LS brine mixes with connate HS water. This aspect is crucial to the progression of the displacement and, moreover, the potential appearance of any LSE – dynamic alteration of wettability is assumed to be correlated to local water salinity and the resultant capillary entry pressure changes perturb the overall pore filling sequence (with implications for oil recovery). Moreover, the coupling of an unsteady-state tracer algorithm allows us to specify a flow-rate for the waterflood: hence, although we are using capillary pressure to control the pore occupancy sequence, we are also implicitly coupling the rate of capillary pressure decline to injection rate.

The 3D pore networks used in this study are assumed to consist of cylindrical pore elements connected by volumeless nodes, and each simulation begins by first defining various network properties: network size (i.e. number of nodes in each direction); pore size distribution (PSD), characterising pore capillary entry radii R; co-ordination number $\bar{Z}$ (a measure of the average connectivity of the pore network); and wettability distribution, characterised for each pore by an effective contact angle θ. The decision to utilise cylindrical pores, and thereby preclude the explicit consideration of film flow, is a very deliberate one; following the work of Sorbie and Collins (2010), we choose to begin our study of LS waterflooding in its simplest incarnation in order to demonstrate the inherent complexity of the subject. Some details regarding potential roles played by film flow in the current approach will be highlighted later in the Discussion section.

Whilst the networks used here are extremely idealised, all of the observations reported later also pertain to more complex network architectures and pore geometries – we are not interested in quantitative prediction at this stage of the modelling, but rather on providing new insights into the LSE itself. The steady-state water-flooding approach has been reported previously (Blunt 1997; Dixit et al. 1999) and proceeds via a step-wise reduction of the capillary pressure P_c, whereby brine entering the system from the inlet face sequentially displaces resident oil-filled pores. Displacement occurs either by snap-off or piston-like mechanisms at the appropriate capillary entry pressure: $\sigma \cdot cos(\theta) / R$ or $2\sigma \cdot cos(\theta) / R$, respectively, where σ is the oil-water interfacial tension (IFT). Note that the snap-off mechanism requires the existence of a water-wet pathway to the inlet, whilst piston-like displacements require bulk water connectivity to the inlet. Isolated oil clusters lacking bulk connectivity to the outlet remain trapped and cannot be mobilised. In each simulation, the P_c is reduced until no further oil in the network can be displaced.

The pore network model described here offers the important opportunity to select the brine injection schedule for any numerical waterflood. For example, it may be desirable to introduce LS brine into a network either at the commencement of the flood (i.e. secondary approach) or at a much later stage of the displacement following a period of HS injection (i.e. tertiary approach). For all simulations performed in this study, we adopt a methodology that captures elements of both – HS brine is injected until water breakthrough, with LS brine injected thereafter. Prior to LS brine injection, when only HS water resides in the pore space, the tracer algorithm is not required to track the salinity within the network. However, following breakthrough, and the first displacement step at which LS is injected, it becomes necessary to effectively "rewind" time and assign appropriate salinities – this is achieved by using an algorithm to track the dispersion of the LS brine associated with the latest saturation change. Note that we have assumed throughout all simulations that pure HS water corresponds to a *tracer* concentration of zero, while pure LS water corresponds to a tracer concentration of one – that is, normalised water *salinity* is effectively equal to *1 - (tracer concentration)*.

Following breakthrough, the existence of a flowing water cluster means that the spatial evolution of brine salinity can be readily tracked. The algorithm that we utilise in this regard comprises two stages: (i) assignment of initial salinities to newly-displaced pores by estimating the salinity of the water driven into them by invading LS brine; and (ii) tracer flow for a time period that accounts for the fact that water egress will increase the *total* volume of injection required to match an increase in network water saturation (i.e. post water breakthrough, not all of the

injected water can be associated with oil displacement – some of it simply bypasses the oil as it flows through the network). Details of this procedure at each displacement step are given below (also see Figure 1 for some typical images showing the evolution of brine salinity as oil is displaced from a network).

Following each decrement in capillary pressure (leading to a new fluid configuration), new salinities are assigned to water-filled pores as follows:

1. Assuming an arbitrary pressure drop between the inlet and outlet faces of the network and Poiseuille flow in each pore, calculate the global pressure solution within the water phase and determine individual bond flow rates.
2. Rescale the above solution to obtain the pressure drop ΔP_{new} required to match the desired fixed injection rate Q.
3. Calculate the overall change in the total volume of water within the network ΔV.
4. Estimate the total length of time $t_{\Delta V}$ required to achieve this volumetric change, according to the following equation (to be discussed below):

$$t_{\Delta V} = \frac{\Delta V}{Q} \cdot \left[\frac{\Delta P_{old}}{\Delta P_{old} - \Delta P_{new}}\right], \tag{1}$$

   where ΔP_{old} is the pressure drop prior to the current displacement step.
5. Before commencing tracer injection, update the tracer concentrations in certain pores according to steps A1 – A4 given in Appendix A. This allows us to predict the initial salinity of water pushed into newly-displaced pores by invading LS brine, and also accounts for saturation changes associated with dead-end branches connected to the backbone of flowing water pores. Using the total mass of tracer M_{tot} assigned during these steps, the time period t_0 allocated to this procedure is given by $t_0 = M_{tot} / Q$.
6. Dynamically update the tracer concentrations in all flowing water-filled pores (see Appendix B for details of the methodology). Adjusting for the period of pre-assignment in step 5, mass conservation stipulates a total tracer injection time of $t^* = t_{\Delta V} - t_0$.

Although this procedure seems rather involved, Equation 1 is the key feature and deserves some further explanation. The term $\Delta V / Q$ equates to the minimum possible time required for *displacement* of the oil-filled pores in the current P_c step, while the second (viscous pressure ratio) term provides an additional factor that quantifies the extent to which this time is increased due to the outflow of water from the network. When reductions in viscous pressure drop between successive P_c steps are large – if a poorly connected spanning water cluster grows, for example – it is assumed that very little water exited the network during the displacement process (i.e. $t_{\Delta V}$ not much larger than $\Delta V / Q$). However, if the water phase is already well-established within the network, only small reductions in viscous pressure can be expected and oil displacement will become highly inefficient (i.e. $t_{\Delta V}$ significantly larger than $\Delta V / Q$; note that a limit is set such that $t_{\Delta V}$ can never be longer than the time required to inject one complete pore volume). Therefore, this formulation produces behaviour that is consistent with typical observations from experimental coreflooding studies. Although a fixed injection rate Q has been

referenced throughout our discussion, it is important to highlight that the recoveries from each simulation are independent of this value – it simply provides a physical time scaling for the LS injection.

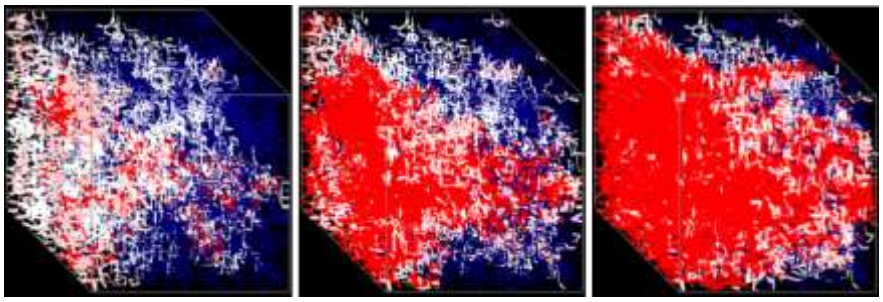

Fig. 1 Snapshots showing a salinity front in a typical simulation where LS water (salinity = 0) displaces oil from a pore network containing HS water (salinity = 1). Normalised salinities represented as follows: red = 0 to 0.25; pink = 0.25 to 0.5; white = 0.5 to 0.75; light blue = 0.75 to 1; dark blue = 1

As mentioned above, the reason for constructing a method to track the water salinity evolution within the network is to investigate the pore-scale impact of dynamic wettability modification by LS (note that the methodology can also be easily adapted to the study of IFT modification). We achieve this alteration to wettability by assuming that the contact angle θ at the entrance of each oil-filled pore is correlated to the local upstream water salinity. In the absence of definitive experimental data regarding the pore-level relationship between brine salinity and wettability within rock structures during LS waterflooding, we base our assumptions upon typical core-level observations from such studies – namely that negligible LSE is seen for injected brine salinities above a certain threshold (roughly 5,000 ppm according to Lager et al. (2006)), but may increase with increasing brine dilutions thereafter (Tang and Morrow 1997; Ashraf et al. 2010). An expression that reflects an increase in the extent of wettability modification with increasing tracer concentration therefore seems reasonable, and for simplicity (as well as ease of analysis) we propose the following Heaviside function for the contact angles of oil-filled pores within the network:

$$\theta = \begin{cases} \theta_{HS}, & C^* < C_{crit} \\ \theta_{HS} \pm \Delta\theta, & C^* \geq C_{crit} \end{cases}, \tag{2}$$

where θ_{HS} is the initial (unmodified) contact angle, $\Delta\theta$ quantifies the extent of contact angle modification (either upwards or downwards, depending on the scenario considered), C^* is the maximum tracer concentration sampled from all neighbouring water-filled pores and C_{crit} is the critical tracer concentration. This formulation reflects an inherent assumption that, upon displacement of a pore with brine of sufficiently low salinity, the oil/rock interface at the entrance of connected pores will be contacted by this brine and a wettability-modifying chemical reaction will occur (e.g. ionic exchange, double layer expansion etc.). Consequently, after each tracer update has completed, the capillary entry thresholds of a range of pores may be altered, and the presence of LS brine in the network may perturb the normal filling sequence that would have taken place in its absence. In summary, this coupled modelling approach provides a novel framework with which to study the significance of such changes to microscopic pore filling and, moreover, assess the likely implications for oil recovery.

3. Results

Given the broad range of apparent inconsistencies reported in the experimental LS waterflooding literature, we resolve to use the current modelling approach to explore the associated parameter space and identify key characteristics of the COBR system that may contribute to the emergence of any LSE. In order to restrict the wide scope of this parameter space and simplify the interpretation of results, in this initial study we choose to focus on networks characterised by homogeneous initial wettability (i.e. networks consist of either 100% water-wet pores or 100% oil-wet pores prior to LS flooding). However, the majority of results to be presented also translate to any network where pores of only one wetting type form a spanning cluster (i.e. the fraction of pores of the other wetting type is smaller than the percolation threshold of the system). Simulations using mixed-wet systems, where both water-wet and oil-wet pores span the network will be presented in a future paper.

Unless otherwise stated, the following base case properties have been utilised for all simulations in this study:

- 30 nodes x 25 nodes x 25 nodes network (with an assumed average pore length of 333 μm, the physical network dimensions are approximately 1 cm x 0.83 cm x 0.83 cm);
- uniform PSD with minimum radius R_{min} = 1 μm and maximum radius R_{max} = 50 μm (note that we select this distribution for ease of analysis: implications for more realistic PSDs are discussed in Supplementary Material);
- $\bar{Z}$ = 5;
- initial water saturation S_{wi} = 0;
- C_{crit} = 0.8 (in the presence of HS brine, this value ensures at least a five-fold dilution is required to elicit local contact angle modification);
- $\Delta\theta$ = 20°.

For each combination of parameters investigated, we perform two separate simulations: the first a standard steady-state displacement with HS injection only; and the second where an initial period of HS injection is followed by LS injection. Generating both sets of results allows immediate interpretation of the overall impact of LS flooding through dynamic contact angle modification. Instead of simply restricting our study to the commonly reported case of increased water-wetness following LS injection, we also provide a thoroughgoing investigation of cases where the system becomes *less* water-wet – a possibility that has gained some credence recently (Fjelde et al. 2012; Shaker Shiran and Skauge 2013). Within the defined parameter space, we can therefore consider ***six*** possible scenarios: ***initially water-wet networks*** becoming (i) more water-wet, (ii) less water-wet, or (iii) oil-wet (i.e. contact angles increase above 90°); and ***initially oil-wet networks*** becoming (i) more oil-wet, (ii) less oil-wet, or (iii) water-wet (i.e. contact angles decrease below 90°). These cases are found to exhibit wide-ranging behaviours and those demonstrating the greatest potential for improved recovery following LS injection will be analysed in depth below.

3.1. Scenario 1: Water-Wet to More Water-Wet

The first case that we consider involves a network of moderate initial water-wetness – where, for simplicity, all contact angles θ_{HS} are assumed to be 60° – that is dynamically modified by LS to become more strongly water-wet (i.e. contact angles are reduced to $\theta_{LS} = \theta_{HS} - \Delta\theta = 40°$ in pores where the local tracer concentration exceeds the critical value C_{crit}). The P_c curve for this simulation, and the corresponding HS injection, are presented in Figure 2. Recalling that the two simulated displacements are identical until water breakthrough (as only HS brine has been injected up to that point), a comparison of these plots reveals some striking features. The introduction of LS is seen to immediately initiate a period of oil recovery at fixed P_c and, overall, much of the oil is seen to be recovered at a higher P_c than previously possible. As we reduce the P_c towards zero, however, the *ultimate* recovery achieved with dynamic contact angle modification is essentially the same as that achieved in its absence. In order to obtain an improved understanding of the mechanisms underlying this behaviour it is necessary to investigate the pore-level physics in greater detail.

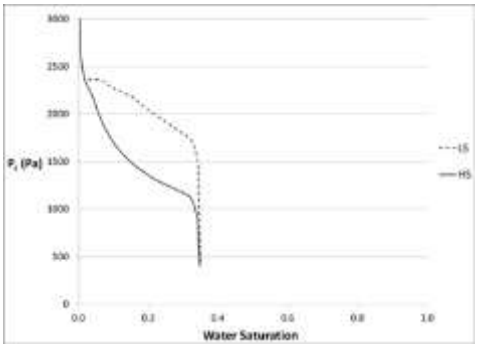

Fig. 2 P_c curves corresponding to Scenario 1 HS (solid line) and LS (dashed line) base case simulations

Plots showing fluid occupancy in pores of different sizes at various time points during the simulations are presented in Figure 3, where pores are labelled as being either water-filled (blue), oil-filled with unmodified contact angle (dark green), oil-filled with modified contact angle (light green) or oil-filled and trapped (red). Since these are imbibition simulations, in the absence of contact angle modification the pores will generally fill in order from smallest to largest according to the defined displacement rules. Once LS enters the network and some contact angles are modified, however, this standard filling sequence can be altered due to the associated changes to capillary entry pressure. Figures 3a and 3b display the pore size fluid occupancies in the HS and LS simulations, respectively, following the first P_c step after water breakthrough. The water and oil occupancies are identical at this stage, but thereafter the two displacements diverge (note that some contact angles have already been modified in the LS case). This is immediately apparent following the next P_c step: in the HS case only some slightly larger (~17 μm) pores are displaced (Figure 3c), whereas the LS has invaded some pores with radii as large as 26 μm (Figure 3d). It is clear, therefore, that the dynamic reduction of some contact angles has led to a significant increase in the accessible pore radius. This behaviour can be easily explained with recourse to some simple analysis of the capillary entry threshold equation.

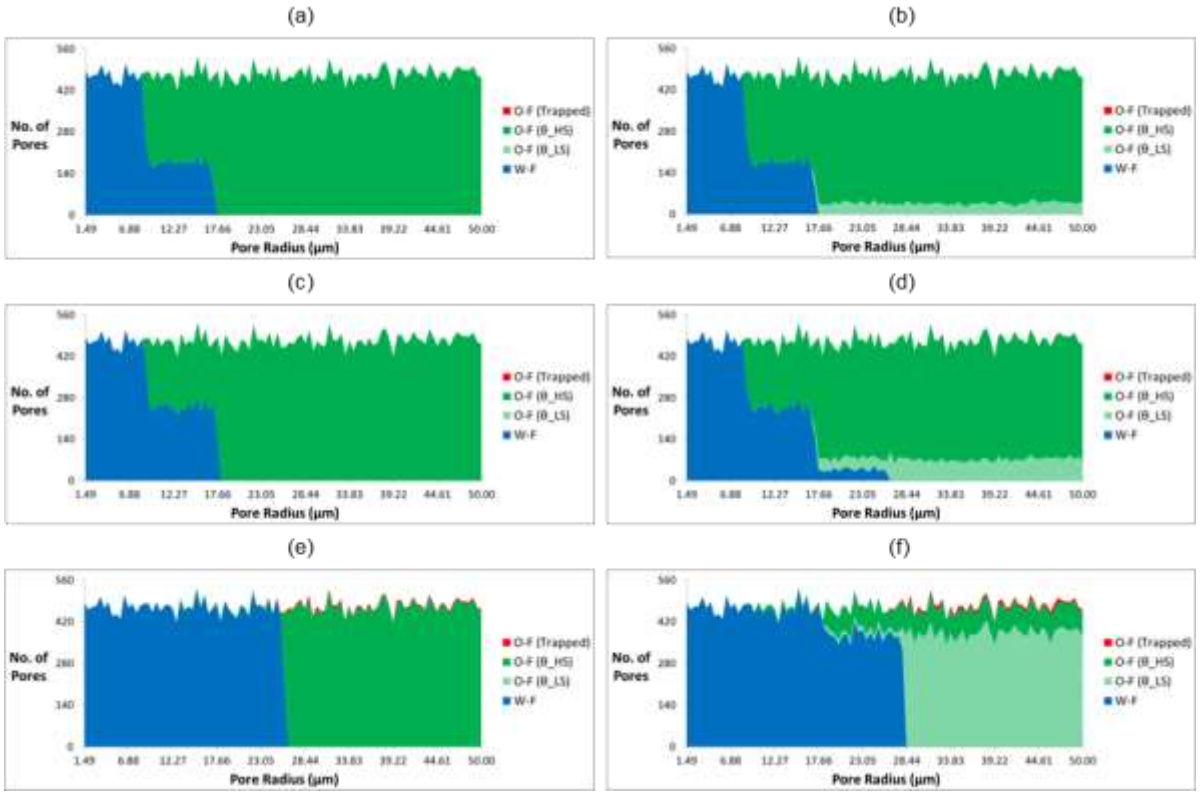

Fig. 3 Plots of pore size fluid occupancy taken during Scenario 1 (a, c, e) HS and (b, d, f) LS base case simulations. Images correspond to the (a, b) first and (c, d) second displacement steps following water breakthrough, and (e, f) the point at which 50% of the pores are water-filled. Pore occupancies represented as follows: blue = water; dark green = oil with unmodified contact angle; light green = oil with modified contact angle; red = trapped oil

For a given P_c value during an imbibition pistonlike displacement, the radius $R_{HS,max}$ of the largest pore that can be displaced in the absence of contact angle modification is:

$$R_{HS,max}(Pc) = \frac{2\sigma\cos(\theta_{HS})}{Pc}, \tag{3}$$

whilst the radius $R_{LS,max}$ of the largest pore that can be displaced with contact angle modification is:

$$R_{LS,max}(Pc) = \frac{2\sigma\cos(\theta_{LS})}{Pc}. \tag{4}$$

Therefore, at a fixed P_c value, these two radii can be related by the expression:

$$R_{LS,max} = \frac{\cos(\theta_{LS})}{\cos(\theta_{HS})} \cdot R_{HS,max}, \tag{5}$$

where $0 \leq \theta_{LS} < \theta_{HS} < \pi/2$ ensures that $R_{LS,max} > R_{HS,max}$. For the above case, therefore, the ratio of the cosines in Equation 5 is approximately 1.53 and this explains why some pores of radius up to 26 μm become immediately displaceable.

Given that contact angle modification can lead to an increased fraction of pores becoming accessible when LS is introduced into the system, the observed period of oil displacement at fixed P_c (c.f. Figure 2) can also now be explained. At this point the displacement essentially undergoes a period of equilibration: without any further reduction in P_c, additional LS injection and contact angle modification means that the displacement "self-reinforces" and fills as many modified pores as possible up to radius $R_{LS,max}$ (and as many unmodified pores as possible up to radius $R_{HS,max}$). The pore size fluid occupancy following the end of this equilibration process is presented in Figure 3f, where, despite the clear differences in pore filling sequence, it is notable that the distribution of water-filled pores is similar to that for the HS case (for equivalent displaced fractions; Figure 3e). Another notable feature of Figure 3f is that, for the remaining oil-filled pores at this stage, the vast majority of contact angles have *already been reduced*. Although it may seem counter-intuitive, as far as increasing *ultimate* oil recovery is concerned this may not be particularly desirable. At this late stage of the LS flood, the system reverts to a case where all contact angles are again identical and this results in the *transient* benefit of LS injection being lost – the pores once again tend to fill in order from smallest to largest (albeit at a higher P_c than would previously have been possible). Therefore, in an identical manner to the HS simulation, the majority of the largest (i.e. > 35 μm) oil-filled pores become trapped before a sufficiently low P_c can be reached that would allow their displacement. The size distributions of water-filled pores are therefore practically identical at the end of the two simulations, making it evident why no *overall* improvement in final oil recovery was observed following LS injection.

A clear shortcoming of the above scenario when attempting to use LS to improve recovery is the failure to make any of the largest oil-filled pores accessible before they become isolated from the network outlet. Inspection of Equation 5 suggests that this could be avoided by increasing the ratio of the cosine terms. There are a number of ways by which this could be achieved: for example, (i) through an increase in $\Delta\theta$ (i.e. giving a smaller θ_{LS} at fixed θ_{HS}), or (ii) by considering a more *weakly* water-wet wettability state prior to LS injection (i.e. assuming a larger θ_{HS} with fixed $\Delta\theta$). P_c curves from HS and LS simulations from a weakly water-wet network with $\theta_{HS} = 75°$ (all other parameters fixed) are presented in Figure 4. The significance of this change is immediately apparent, with Figure 4a demonstrating that LS injection gives an increase in overall recovery of around 8.5% compared to the HS case. Note that the ratio of cosines for this case is approximately 2.22. Hence, LS injection immediately allows some pores with radii up to 38 μm to be displaced. This modification in accessible pore radius is much larger than that seen in the base case simulation and, consequently, leads to an extended period of self-reinforcing water ingress at fixed P_c. This radius is larger than the 35 μm trapping threshold identified in the base case simulation, and so, by simply reducing the initial water-wetness of the network, LS injection has led to the displacement of a number of larger pores that were previously inaccessible.

Crucially, however, the observed increase in oil recovery is not simply the result of a more volumetrically favourable pore filling sequence: Figure 4b also indicates an improvement in displacement efficiency, with LS injection allowing an additional 5% of pores to be invaded. To achieve this necessarily requires a reduction in topological oil trapping and to understand the mechanism responsible for this result, it is necessary to examine the progression of the displacement within a *spatial* context. Fluid occupancy plots, illustrating the spatial progression of pore filling at different positions between the network inlet and outlet, are presented in Figure 5

for both the HS and LS displacements (note that the colour scheme is consistent with the pore size plots in Figure 3). Beyond water breakthrough, the HS case shows negligible spatial variation, with pores largely displaced uniformly across the network at all times (Figures 5a, c and e). The LS case is remarkably different, however, with displacement events occurring in a wave from the inlet to the outlet in response to an evolving front of contact angle modification created by the invading LS (Figures 5b, d and f). This allows for a more efficient sweep of the pore space: many pores towards the inlet are displaced "earlier" (i.e. at a higher P_c) than would have been possible in the absence of LS, thus reducing the prevalence of trapping that inevitably occurs as bulk oil connectivity to the outlet is reduced. A similar front of contact angle modification was seen to progress across the network in the base case LS simulation; however, since far fewer capillary entry thresholds were satisfied during this process, only a very weak concurrent front of oil displacement was observed. Evaluating these two sets of results, which were obtained using different θ_{HS} values, we can conclude that *the initial rock wettability is likely to be one of the key parameters in determining whether or not a beneficial LSE will be seen for a particular COBR system.*

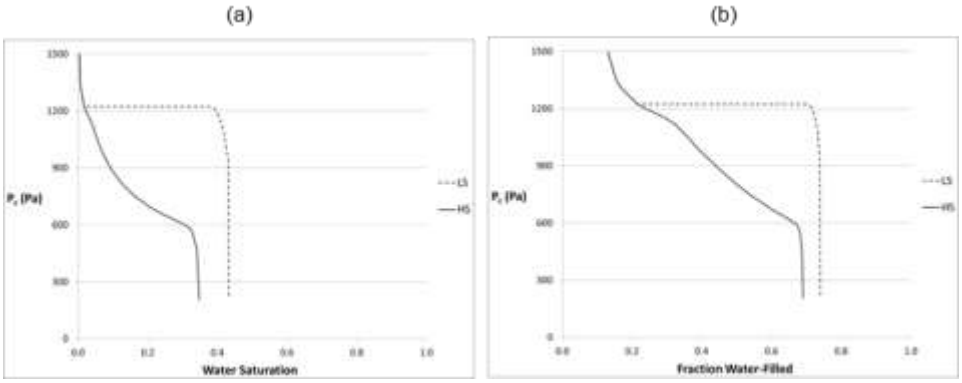

Fig. 4 P_c plotted against (a) water saturation and (b) fraction of pores water-filled for Scenario 1 HS (solid lines) and LS (dashed lines) sensitivity simulations with $\theta_{HS} = 75°$

The expression given in Equation 5 also reveals a further factor that can play a crucial role in determining the extent of any LSE. Although not immediately apparent, the relationship between the particular $R_{LS,max}$ and $R_{HS,max}$ values and the network PSD is found to be extremely important. This is due to the fact that the ratio R_{max} / R_{min} effectively controls the fraction of oil-filled pores that potentially become accessible at P_c values below that at which LS injection commenced. If this ratio is large, $R_{LS,max}$ will be much smaller than R_{max} and none of the largest pores will become accessible at the prevailing P_c; conversely if the ratio is small, $R_{LS,max}$ may exceed R_{max} and all of the pores in the network will potentially become accessible at the current P_c. Naturally, this latter case can lead to an extremely efficient sweep of the pore space, with very few oil-filled pores left trapped in the network (see Supplementary Material for a sensitivity simulation using a uniform PSD with $R_{min} = 50$ μm and $R_{max} = 100$ μm). Our predictions are supported by recent experimental coreflooding results that indicate a correlation between average pore-throat radius and incremental oil recovery achieved by LS injection (Shehata and Nasr-El-Din 2014). *This suggests that the PSD should be a key consideration when attempting to identify good candidates for LS injection.*

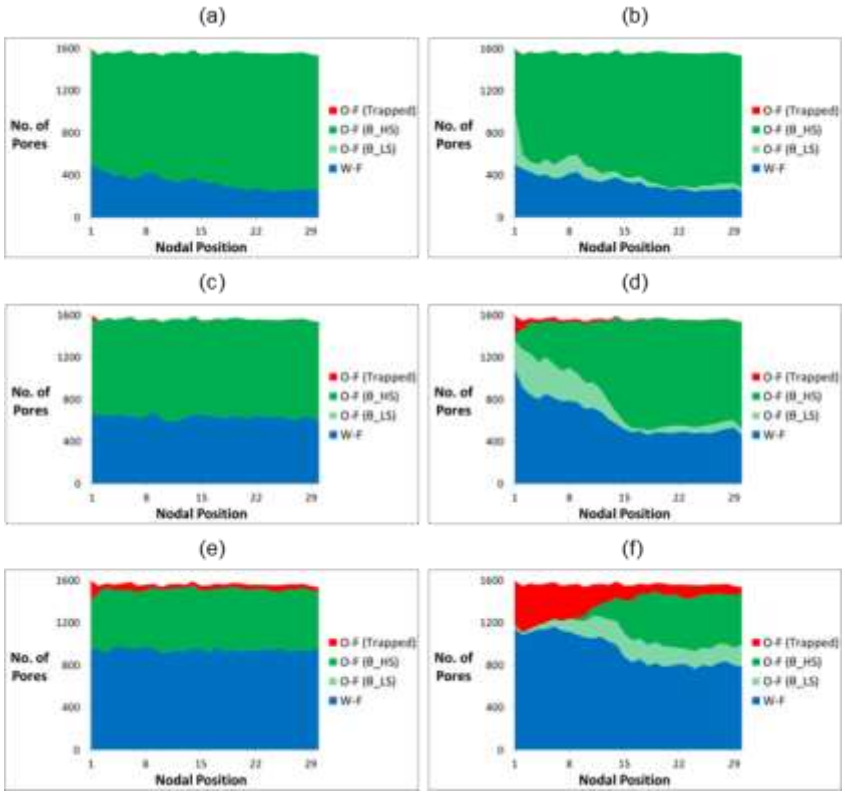

Fig. 5 Plots of spatial fluid occupancy taken during Scenario 1 (a, c, e) HS and (b, d, f) LS sensitivity simulations with θ_{HS} = 75°. Images correspond to (a, b) the first displacement step following water breakthrough, and the points at which (c, d) 40% and (e, f) 60% of the pores are water-filled

In this section, we have analysed the process of dynamic contact angle reduction by LS injection in uniformly water-wet networks. The initial wettability, extent of wettability alteration and rock PSD have been recognised as critical parameters, with favourable combinations potentially improving recovery (compared to HS injection alone) by producing efficient displacements that recover oil from otherwise inaccessible large pores. In general, we can conclude that LS injection is favourable in this scenario – the worst possible outcome was demonstrated in the base case simulation, where, although the filling *sequence* was seen to be significantly altered by LS, the distribution of trapped oil pores remained unaltered.

3.2. Scenario 2: Oil-Wet to Less Oil-Wet

Having studied the reduction of contact angles by LS injection in uniformly water-wet networks, we now proceed to examine the corresponding oil-wet case. We begin by considering a strongly oil-wet network, having contact angles θ_{HS} of 140°, and assume that dynamic modification by LS leads to a change towards more moderate oil-wetness (i.e. θ_{LS} = 120°). To facilitate comparisons with the results from Scenario 1, these θ_{HS} and θ_{LS} values have been selected such that the respective cases are equivalent (i.e. $|cos(40°)| \equiv |cos(140°)|$ and $|cos(60°)| \equiv |cos(120°)|$). The base case HS and LS P_c curves for this scenario are presented in Figure 6. Although the displacement is now a drainage taking place under negative P_c conditions, and pores therefore tend to fill in a largest-to-smallest sequence, the qualitative features of the results with LS injection strongly resemble those of the base case imbibition of Scenario 1. Following the introduction of LS, we see more oil recovered at a higher P_c and a period of self-reinforcing saturation change, but again there is no improvement in the *overall* oil recovery.

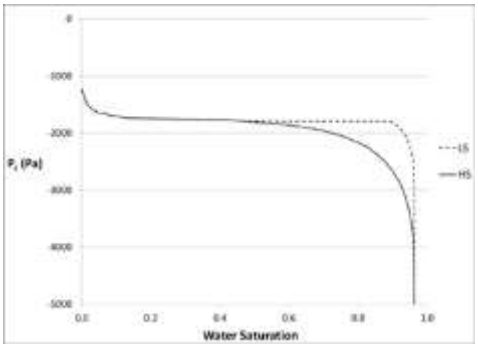

Fig. 6 P_c curves corresponding to Scenario 2 HS (solid line) and LS (dashed line) base case simulations

These results strongly suggest the mechanisms of action of LS here to be rather similar to those identified in Scenario 1. In order to investigate this theory, it is instructive to derive an equivalent expression to Equation 5 for drainage displacements. In this case, for a given P_c value, we can define:

$$R_{LS,min} = \frac{\cos(\theta_{LS})}{\cos(\theta_{HS})} \cdot R_{HS,min}, \tag{6}$$

where $R_{HS,min}$ and $R_{LS,min}$ are the radii of the smallest pores that can be displaced in the absence and presence of contact angle modification respectively, and $\pi/2 < \theta_{LS} < \theta_{HS} \leq \pi$ ensures that $R_{LS,min} < R_{HS,min}$.

In the base case simulations presented in Figure 6, water breakthrough occurs with HS water capable of accessing pores with radii down to ~34 µm. Since, from Equation 6, $R_{LS,min} = 0.65 \cdot R_{HS,min}$, subsequent wettability alteration by the introduction of LS allows invasion of pores with radii as small as ~22 µm – this modification in accessible pore radius is again responsible for the observed self-reinforcement period at fixed P_c in the LS simulation. Reflecting the behaviour of the base case simulation from Scenario 1, in the aftermath of this saturation shift, a standard (largest-to-smallest) filling sequence resumes because the majority of remaining oil-filled pores have already undergone contact angle modification. As a consequence, in both the HS and LS simulations, the smallest (i.e. < 15 µm) oil-bearing pores become trapped before a sufficiently negative P_c can be reached that would allow their displacement. This result is confirmed by Figure 7, where the size distributions of water-filled pores are equivalent at the end of the respective HS and LS simulations.

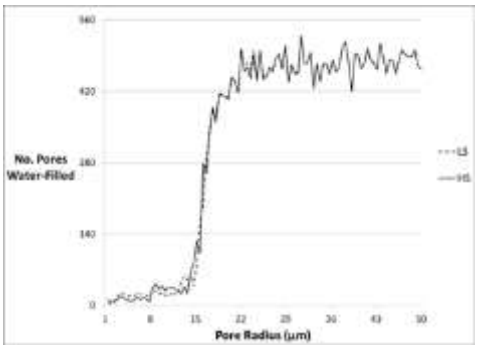

Fig. 7 Size distribution of water-filled pores at residual oil saturation in Scenario 2 HS (solid line) and LS (dashed line) base case simulations

Although no additional oil is ultimately recovered at the end-point P_c in this case, the similarities between Equations 5 and 6 make it clear that the same parameters are critical to the performance of LS in both the water-wet and oil-wet cases – namely, the initial contact angle, the extent of dynamic wettability alteration and the rock PSD. Sensitivity simulations confirm this to be true, but clear differences in pore-scale behaviour are often found to exist between equivalent water-wet and oil-wet networks following LS injection. Therefore, a more thorough investigation of the nature of the associated modifications to accessible pore radius is merited. Simple manipulations of Equations 5 and 6 reveal that the absolute differences between the particular limiting radii vary with the current P_c in each case. For water-wet networks we have:

$$\left|R_{HS,max}(Pc) - R_{LS,max}(Pc)\right| = R_{HS,max}(Pc) \cdot \left|1 - \frac{\cos(\theta_{LS})}{\cos(\theta_{HS})}\right|, \quad (7)$$

while for oil-wet networks:

$$\left|R_{HS,min}(Pc) - R_{LS,min}(Pc)\right| = R_{HS,min}(Pc) \cdot \left|1 - \frac{cos(\theta_{LS})}{cos(\theta_{HS})}\right|. \quad (8)$$

Importantly, in each case the magnitude of the capillary entry radius modification following LS injection is seen to be proportional to the radius of the largest or smallest pore that can be displaced in the absence of contact angle reduction (i.e. $R_{HS,max}$ or $R_{HS,min}$, respectively). As an imbibition simulation proceeds, $R_{HS,max}$ gradually increases and, hence, so does the magnitude of the entry radius modification; conversely, as a drainage simulation proceeds, $R_{HS,min}$ is gradually reduced and so the degree of modification is diminished. In other words, the fraction of potentially accessible oil-filled pores following LS injection, compared to HS injection alone, may *increase* during imbibition in water-wet networks but *decrease* during drainage in oil-wet networks. This raises an important question regarding the optimum timing of LS injection under certain wettability conditions.

In summary, we have demonstrated that the pore-scale mechanisms associated with improved oil recovery following dynamic contact angle *reduction* by LS injection are largely conserved between water-wet and oil-wet networks. Much like the equivalent water-wet case, LS injection into oil-wet networks can be deemed to be favourable under certain conditions – the worst case scenario involves both the HS and LS simulations displacing roughly the same pores with no additional recovery achieved.

3.3. Scenario 3: Oil-Wet to Water-Wet

With regard to dynamic reduction of contact angles following LS injection, the final case that we consider involves the wettability alteration of a weakly oil-wet network (i.e. θ_{HS} = 100°) towards weak water-wetness (i.e. θ_{LS} = 80°). Simulated base case P_c curves from the HS and LS simulations are presented in Figure 8 and exhibit a very modest 2% increment in overall oil recovery following LS injection (Figure 8a). This small volumetric increase is, however, not the key aspect of the comparison: upon inspection of Figure 8b, it can be seen that a highly efficient *sweep* of the pore space has been achieved. The introduction of LS has resulted in strong self-reinforcement during the displacement and 97% of the oil-filled pores have been invaded without any further reduction in P_c. Remembering that the simulation begins as a drainage displacement – where the P_c is negative from the outset – this striking result is easily explained: when LS water induces contact angles to decrease below

90°, the capillary entry pressures of modified pores become positive and, hence, these pores can be immediately imbibed regardless of their specific radii. As a result, the concept of a radius-related filling sequence becomes irrelevant and the displacement is driven purely by the spatial evolution of LS within the pore space. A well-defined front of contact angle modification passes across the network, closely followed by a front of oil displacement, ultimately leaving very few oil-filled pores unswept.

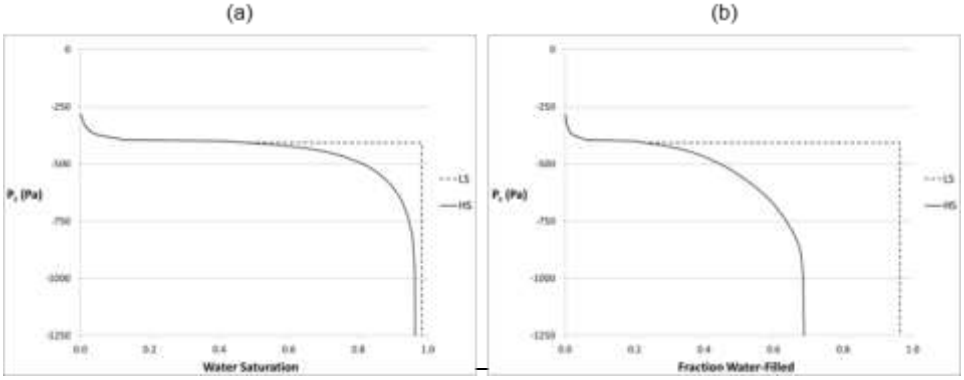

Fig. 8 P_c plotted against (a) water saturation and (b) fraction of pores water-filled for Scenario 3 HS (solid lines) and LS (dashed lines) base case simulations

Due to the mechanisms governing the LS flood in this scenario, it is crucial to note that an extremely efficient sweep will be observed for all parameter combinations (provided the respective HS and LS contact angles lie either side of 90°). It should be emphasised, however, that the extent of incremental oil recovery will still depend on the particular PSD used. Since any additional oil produced as a result of LS injection arises from the displacement of small pores that would not be accessed by HS alone, the overall *volumetric* benefit will increase as the variance of the individual pore volumes in the network decreases. This explains the small 2% improvement in recovery seen in the base case, where R_{min} = 1 µm and R_{max} = 50 µm (which defines a wide range of volumetric (~R^2) values). A sensitivity simulation using a narrower volumetric distribution, R_{min} = 50 µm and R_{max} = 100 µm, has been found to produce a much more significant incremental LS recovery of 19%. Thus, although some simulations may predict only small increases in recovery in this scenario, it can be concluded that LS injection is always extremely favourable when contact angles cross over from oil-wet to water-wet values.

3.4. Scenario 4: Water-Wet to Oil-Wet

Although it is commonly believed that LS injection into a COBR system can lead to an increase in water-wetness, there remain only a handful of cases where this phenomenon has been directly measured (Patil et al. 2008; Agbalaka et al. 2009). The current model therefore provides a valuable tool with which to consider the full range of behaviours that may result from dynamic wettability alteration in general. With that in mind, we now investigate a case that is effectively the mirror image of Scenario 3: an initially weakly water-wet network, with all contact angles θ_{HS} = 80°, is dynamically modified by LS injection to become weakly oil-wet (i.e. θ_{LS} = 100°). As indicated by the P_c curves generated for LS injection with the base case parameters (Figure 9), this dynamic switching of wettability introduces a drainage leg to the curve, since some pores cannot now be displaced until a sufficiently *negative* P_c is reached (note that a self-reinforcing equilibration period at fixed P_c is not a possibility in this case). We observe that LS injection is detrimental to oil recovery while the capillary pressure remains

positive, but it becomes highly beneficial if negative capillary pressures can be achieved. To fully understand the pore-level mechanisms effecting these results, we again require consideration of both spatial influences and the relative entry thresholds of pores with modified and unmodified wettability as the P_c is gradually reduced.

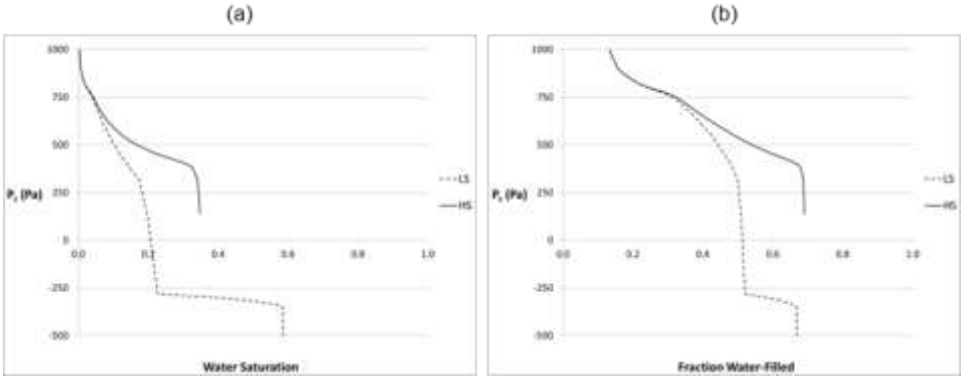

Fig. 9 P_c plotted against (a) water saturation and (b) fraction of pores water-filled for Scenario 4 HS (solid lines) and LS (dashed lines) base case simulations

In comparison to the previous cases, where LS injection was assumed to reduce contact angles, the spatial evolution of water salinity within a network is found to be rather different when LS induces increased oil-wetness. When LS first enters the network and contact angles of some neighbouring pores are increased, the local fraction of imbibable pores is immediately diminished; the displacement can then only continue by accessing water-wet pores downstream from the invading LS. By displacing these pores, however, LS water is accelerated downstream and local oil-filled pores are once again "shut-off", forcing the cycle to repeat. This can lead to a rather disorganised pattern of contact angle modification, and, unlike the scenario with dynamic contact angle reduction, it is much less likely that a discernible front of contact angle modification will progress across the network. Moreover, an unfortunate consequence of this process is that pores with unmodified contact angles (most likely found downstream) may be displaced more readily than pores with modified contact angles (most likely found upstream). This can enhance the likelihood of water fingering that creates isolated oil clusters upstream and explains the slight increase in the fraction of trapped pores when injecting LS rather than HS (Figure 9b). The additional 24% of oil recovered when injecting LS compared to HS (Figure 9a) can, therefore, only be explained by a volumetrically favourable alteration to the pore filling *sequence*.

A further feature not observed in Scenarios 1-3, but common to cases where LS injection increases oil-wetness, is the emergence of two separate pore filling sequences – displacing, respectively, pores with modified and unmodified contact angles. In the present scenario, these two sequences proceed in opposite directions: water-wet pores, unmodified by LS, fill from smallest to largest, whilst the newly oil-wet pores are eventually displaced in a *largest-to-smallest* sequence. The result of this phenomenon can be observed in Figure 10, which presents the size distribution of water-filled pores at the end of the respective HS and LS simulations. When LS brine is introduced (following water breakthrough) and the P_c is gradually reduced, unmodified water-wet pores of increasing radius are sequentially displaced. At the same time, an increasing number of the (primarily larger) oil-filled pores in contact with LS brine have their contact angles increased beyond 90º, with the result that the *cumulative number of oil-wet pores in the system increases with decreasing* P_c. Once the imbibition of all

remaining water-wet pores has been completed (P_c = 0), the pressure in the water phase is increased and the drainage leg of the flood begins – now, the largest oil-wet pores fill first. The result of this substantially altered filling sequence is the trapping of oil pores with radii mostly in the range (20, 40) μm – a more volumetrically favourable outcome than the HS displacement, where pores mostly in the range (35, 50) μm remain trapped.

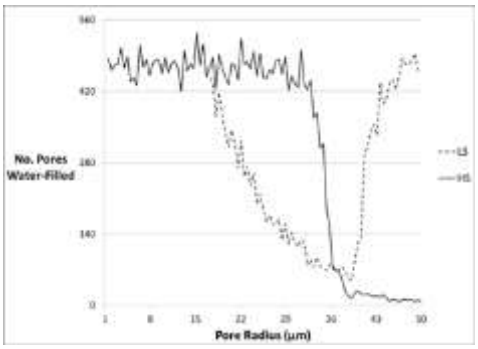

Fig. 10 Size distribution of water-filled pores at residual oil saturation in Scenario 4 HS (solid line) and LS (dashed line) base case simulations

In a similar manner to Scenario 3, the ultimate oil recovery obtained under the current assumptions is independent of the particular choice of θ_{HS} and θ_{LS} values – provided they sit either side of 90°, the outcome will always be the same. This is due to the clear separation of the filling sequences that are created (i.e. *imbibition* of pores with unmodified contact angles and *drainage* of pores with modified contact angles). However, the incremental recovery achieved by LS injection *is* still sensitive to PSD parameters. Although the LS mechanisms responsible for improved recovery are insensitive to the particular distribution of pore radii, the nature of the modified filling sequence means that increasing the *variance* of the individual pore *volumes* will affect incremental oil recovery. If pore volumes are widely distributed, then the volumetric improvement in oil recovery – achieved by displacing the largest pores in the network at the expense of some smaller pores – will tend to exceed that obtained for a narrower range.

The fact that this scenario can lead to significant improvement in oil recovery is of particular significance, since a number of studies have indicated that LS brine may indeed lead to wettability alteration towards more oil-wet conditions – rather than the more commonly suggested phenomenon of increased water-wetness (Buckley et al. 1997; Fjelde et al. 2012; Shaker Shiran and Skauge 2013). *Provided a sufficiently negative P_c can be achieved to displace newly oil-wet pores*, the injection of LS is predicted to be very favourable in this scenario. This is due to a positive volumetric effect: dynamically introducing a drainage leg allows displacement of the very largest pores in the network, which would usually be trapped using HS alone.

4. Discussion

The technique of LS injection has been widely investigated over recent years, with both core- and field-scale studies examining its apparent potential to improve oil recovery compared to conventional waterflooding. Whilst positive outcomes have been frequently reported, this has not always been the case and, thus far, a clear understanding of the key factors underlying such results is yet to be established. In this paper, a novel pore

network modelling approach has been developed, with the aim of bringing some clarity to this situation by examining a range of parameters that may influence the pore-scale displacement behaviour following LS injection. Critical to this *in silico* approach is the decision to neglect explicit consideration of chemical reactions in the COBR system, and instead assume that LS invasion leads to dynamic local modification of rock wettability. From a physical standpoint, this assumption is reasonable, since wettability alteration is a phenomenon commonly believed to accompany LS flooding in a variety of reported coreflooding studies.

In order to explore the associated parameter space in a computationally-efficient manner, we have chosen to adopt a P_c-driven steady-state approach to the problem and developed an innovative tracer approach to estimate the spatio-temporal evolution of water salinity following each step of LS injection into HS-bearing networks. The model assumes that a critical local salinity must be reached for wettability alteration to occur, and this condition is used to identify individual pores for contact angle modification. As has been clearly demonstrated by the model, the dynamic nature of this process, when combined with certain parameter values, has the ability to significantly alter pore-level displacement sequences and, consequently, the ultimate oil recovery from networks with uniform initial wettability.

The assumptions we have made regarding contact angle modification in response to invading LS brine can be seen to have a strong resemblance with those presented previously in the pore-scale theory of Sorbie and Collins (2010). We regard their study as an important pre-cursor to the current work and, whilst their study did not probe the associated COBR parameter space quite so extensively, it remains worthwhile to highlight some key consistencies between the reported results. Both studies identify, for example, a lack of potential for improved LS recovery in strongly water-wet networks and also demonstrate that, in general, only small alterations to wettability may be necessary to elicit significant improvements in oil recovery. Our inclusion of explicit fluid transport within the pore network, however, significantly broadens the scope of the approach and identifies phenomena that would have been difficult to predict using their simplified approach. Our model clearly demonstrates, for example, the crucial role played by the PSD, and the manner in which this can be implicated in the improvement of sweep efficiency during LS waterflooding.

Having chosen to neglect explicit models for film flow, we nevertheless still find the modelling capable of predicting rich and complex pore-level behaviour. However, it is worthwhile considering the potential implications of including film flow mechanisms in the approach. Corner flow could, for example, be included as a transport mechanism for the injected LS brine; however, since at this stage we only consider LS invasion following breakthrough, we believe that flow through the spanning bulk pathways would be the dominant transport mechanism. A further film flow-related possibility is the potential drainage of corner oil from oil-wet pores in response to local changes in brine salinity. Consider, for example, a triangular pore in which HS water and oil layers remain in the corners following HS flooding, where the extent of the oil layer will depend on the local capillary pressure. In the context of this work, two relevant cases exist where subsequent LS invasion could produce additional corner oil: (i) Scenario 2, where menisci may push further into the pore corners to maintain consistency with the modified capillary pressure; and (ii) Scenario 3, where *all* oil may ultimately be removed

from the layers. In general, however, we note that the contribution of such oil drainage to the overall recovery is unlikely to be as significant as the incremental oil produced by the bulk displacement mechanisms.

In the experimental literature, it is most commonly reported – often without direct justification – that the injection of LS into a COBR system leads to a movement towards increased water-wetness of the rock, and that any incremental oil recovery arises as a result of this wettability alteration mechanism. All three comparable cases (c.f. Scenarios 1-3) investigated in this study go some way towards corroborating this hypothesis: dynamic reduction of contact angles following LS injection, accompanied by corresponding increases in capillary entry pressures, is generally found to be favourable compared to conventional HS flooding as more efficient sweeps of the pore space become possible. Notably, however, a number of studies have also reported evidence of contrasting behaviour – that is, a movement towards increased oil-wetness following LS injection – and this possibility has also been investigated (c.f. Scenario 4). In contrast to the case of dynamic changes towards increased water-wetness, any potential benefit of LS in systems that become *less* water-wet depends strongly on the initial and final wettability conditions of the network. Generally speaking, we can conclude the following: (i) initially oil-wet networks that become more oil-wet show no potential for improved recovery following LS injection (results not shown); (ii) initially water-wet networks that become less water-wet show some potential (results not shown); (iii) most significantly, initially water-wet networks that become oil-wet show strong LS potential compared to conventional HS flooding. This potential variability in outcomes is reflected in recent experimental studies, where a LS-induced increase in oil-wetness has been identified by numerical history matching of experimental coreflooding data: Sandengen et al. (2011) reported a negative LSE (possibly reflecting case (i) above), while Shaker Shiran and Skauge (2013) observed a case with markedly improved recovery. This latter case is of particular significance, and our simulations corresponding to case (iii) demonstrate the existence of a key mechanism that may contribute to explaining the result – specifically, the displacement of some otherwise inaccessible large pores due to the invasion of a fraction of smaller pores either being delayed or prevented altogether.

Considering the results from all simulated scenarios, two key pore-scale mechanisms emerge that would appear to control any observed variation in oil recovery following dynamic wettability modification during LS waterflooding: (a) the "sweep efficiency effect", whereby differences in the overall *fraction* of the pores displaced by LS are observed compared to conventional HS flooding; and (b) the "filling sequence effect", whereby an alteration to the standard HS pore filling *sequence* can impact the overall amount of oil produced. It is important to note that these two effects are not necessarily mutually exclusive and the overall outcome of any LS flood will depend on the relative (scenario-dependent) influence of each mechanism. See Table 1 for a quantitative summary of the evolving water saturations during each presented simulation.

One of the key objectives at the outset of this study was the identification of parameters that may contribute to improved oil recovery by the LSE. In Scenarios 1 and 2, the combination of initial wettability and magnitude of wettability alteration has been recognised as critically important – principally through the parameter grouping $cos(\theta_{HS} - \Delta\theta) / cos(\theta_{HS})$. Increasing the absolute value of this ratio has been shown to open up the possibility of improved sweep efficiency by increasing the fraction of pores in a network that potentially become accessible

upon the introduction of LS brine. In practice, this relates to the modification of individual contact angles by LS, with a subset of previously inaccessible pores attaining capillary entry pressures that exceed the current P_c. There exist two ways by which this cosine ratio could be increased, namely: (a) increasing the LS-induced change in contact angle $\Delta\theta$, or (b) beginning with more neutral-wet conditions (i.e. θ_{HS} closer to 90°). From an experimental point of view, the first of these could likely be achieved by decreasing the salinity of the injected water; indeed, additional improvement in overall recovery is frequently reported in the coreflooding literature when results with water of low salinity are compared to those with water of even lower salinity (Tang and Morrow 1997; Patil et al. 2008; Ashraf et al. 2010). The implications of the second mechanism are also noteworthy, suggesting that uniformly-wetted networks that are either very strongly water-wet or oil-wet may be poorer candidates for LS injection than somewhat more weakly-wetted counterparts.

Scenario	θ_{HS}	θ_{LS}	Final Water Saturations			Intermediate Water Saturations		
			HS	LS	Increment	HS	LS	Increment
1	60°	40°	0.347	0.349	0.002	0.221	0.344	0.123
1	75°	55°	0.347	0.432	0.085	0.221	0.432	0.211
2	140°	120°	0.963	0.964	0.001	0.926	0.962	0.036
3	100°	80°	0.963	0.984	0.021	0.926	0.982	0.056
4	80°	100°	0.347	0.592	0.245	0.347	0.421	0.074

Table 1 Summary of the water saturations and corresponding incremental oil recoveries observed during the simulated HS and LS waterfloods for each combination of initial and modified wettability. Final water saturations reflect those at the very end of each displacement, whilst intermediate saturations were obtained in each case at the P_c at which 60% of the pores had been water-filled in the network with larger contact angles. The notable discrepancies between incremental recoveries at these two simulation stages serve to highlight the fact that apparent LS efficacy can depend strongly on the end-point P_c achieved during a particular flood.

The second factor found to be crucial in determining the extent of any LSE in a network is the particular distribution of pore sizes. In Scenarios 1 and 2, the PSD has been shown to be critical in determining any increase in sweep efficiency following LS injection. In a network having pore radii uniformly distributed between R_{min} and R_{max}, a decrease in the ratio R_{max} / R_{min} has been shown to lead to an increase in the fraction of pores that potentially become accessible after LS injection. As this ratio is reduced, the overall range of capillary entry pressures of oil-bearing pores becomes smaller and, hence, an equivalent reduction in contact angles leads to a larger subset of previously inaccessible pores having their entry pressures modified above the prevailing P_c. In addition, for more realistic PSDs, such as those of truncated normal type, sweep efficiency has been found to increase with both decreasing pore size variance and increasing mean pore size (c.f. Supplementary Material). This latter result corroborates data recently reported by Shehata and Nasr-El-Din (2014) in a waterflooding study utilising sandstone core plugs of various permeabilities.

The form of the PSD has also been shown to be of great importance in Scenarios 3 and 4 – in these cases, however, the PSD has no influence on sweep efficiency *per se*, and its significance instead relates to the *volumetric* consequences for overall oil recovery following dynamic wettability modification. The relative gain in oil recovery arising from water-wet pores becoming oil-wet is more significant when the variance in individual pore *volumes* is large – that is, when very large, newly oil-wet pores are displaced at the expense of very small, newly oil-wet pores. The opposite result is true when LS causes the pores of an oil-wet network to become water-wet: if the variance in individual pore volumes in this case is very narrow, a more efficient sweep of the smallest pores – due to reduced topological trapping – will produce a significant amount of previously unavailable oil.

Although the modelling approach considers dynamic wettability modification to be the dominant LSE mechanism, the demonstrated importance of the rock PSD may have wider implications. Tiny clay particles are sometimes observed in fluid effluent during experimental LS injection studies in sandstone core samples, and this has led to the hypothesis that fines migration may play a significant role in increasing oil recovery. Whilst the blocking of individual pores and subsequent microscopic diversion of flow may be a factor in determining LS efficacy, the results from this study suggest that the modification of individual pore sizes – and, hence, the effective PSD – by swelling, stripping and downstream deposition of small particles could also be very important.

Throughout this paper we have frequently measured the success of a LS waterflood by comparing the *ultimate* oil recovery (or displaced pore fraction) with that achieved by an equivalent HS flood. Employing this metric, however, inherently assumes that the required minimum P_c can always be attained, and thus it is crucial to highlight the implications in circumstances where sufficient water drive cannot be achieved. Figure 11 demonstrates how the incremental recovery by LS injection varies with P_c over the course of each base case simulation. Those corresponding to initially water-wet networks (Scenarios 1 and 4) are given in Figure 11a, whilst those from initially oil-wet networks (Scenarios 2 and 3) are given in Figure 11b – note that the x-axes have been reversed such that the time course of each simulation runs from left to right along the plots. The key point to emphasise here is that if the minimum P_c is not reached in a particular case, then any assessment of the overall LS benefit could potentially be misleading. For example, if the end-point P_c in Scenario 2 happened to be above the minimum value, a sizeable incremental recovery following LS injection could be observed. However, the production of this "additional" oil would simply reflect that a greater volume of *untrapped* oil remains immobile in the HS flood due to the action of capillary forces. Conversely, in cases where contact angles are dynamically increased, the potential benefit of LS injection could be *under*-predicted. A diminished recovery is seen in Scenario 4 while the P_c is positive, but, following the invasion of newly oil-wet pores at negative P_c, a significantly improved recovery emerges. Unfortunately, the current steady-state modelling approach cannot be used to *predict* the likely end-point P_c in a particular flood; however, these observations serve to highlight that caution should be exercised in the interpretation of experimental LS coreflooding data. Depending on the distribution of viscous and capillary forces within a particular core, it seems possible that an apparent LSE (or lack of) could simply arise as an artefact of the underlying experimental protocol.

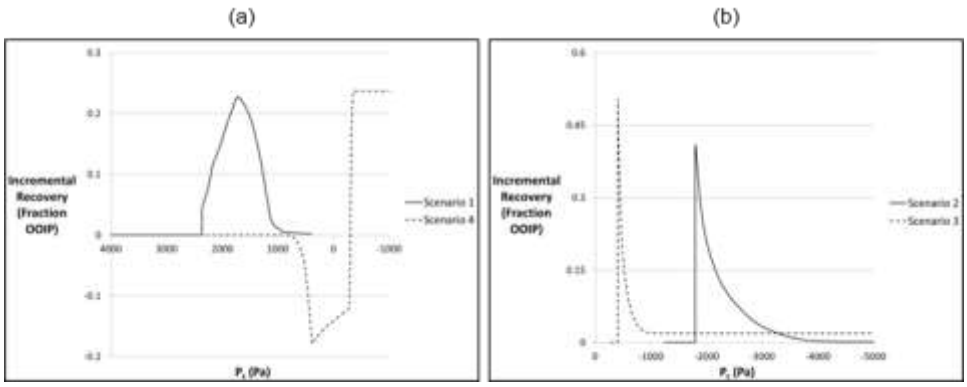

Fig. 11 Difference between HS and LS base case oil recoveries plotted against P_c for corresponding displacements in initially (a) water-wet and (b) oil-wet networks. Cases represented as follows: Scenarios 1 and 4 = solid lines; Scenarios 2 and 3 = dashed lines

One of the key issues highlighted by this modelling study is that the wide range of seemingly contradictory results reported in the experimental literature should be far from surprising. Even with the development of a relatively simple steady-state displacement model and restricting investigations to a small region of parameter space, a broad range of possible behaviours following LS injection has been demonstrated. Importantly, this is not to say that the mechanisms underlying experimental results are too complex to be understood, but simply that additional parameters must be measured in order to critically assess the outcomes. In this study, we have shown that the initial wettability state of the system, the extent of wettability alteration due to LS brine, and the rock PSD are all critically important in determining whether or not improved oil recovery will be observed following LS injection. Although various experimental protocols are available to measure or estimate such parameters, very few studies have considered these in the interpretation of their data.

Of course, we have focussed here only on systems of uniform wettability and we have adopted a relatively modest modelling methodology that sits somewhere between steady-state and unsteady-state approaches (and between secondary and tertiary LS applications). However, our results have highlighted a number of key areas for further research – both experimental and numerical – and we believe that this pore network modelling framework will prove to be extremely valuable in identifying additional parameters that are critical to LSE and, moreover, help to clarify the prevailing uncertainty in the LS coreflooding literature.

Appendix A: Salinity allocation to newly-invaded pores

The following procedure is used to assign salinity values to each pore newly invaded during the latest capillary pressure step:

A1. Identify newly displaced water-filled pores without bulk connectivity to the inlet (i.e. snapped-off pores). These pores are assumed to have accumulated pure HS water and assignment of a non-zero tracer concentration is delayed until any such pore becomes part of a spanning water cluster.

A2. Assign a tracer concentration of one (i.e. salinity = 0) to all newly displaced inlet pores.

A3. Beginning from the inlet, track flow paths through the spanning water cluster(s) and assign tracer concentrations to all *newly* displaced, or *newly* connected, flowing pores according to the flow-weighted average concentration of upstream neighbours.

A4. Identify "dead-end" water clusters (i.e. pores branching from a backbone of flowing water pores but not yet flowing themselves), and non-spanning water clusters with bulk connectivity to the inlet. For each of these clusters, calculate the total cluster volume V_{clus}, the total mass of tracer newly added to the cluster M_{new} (i.e. pores *just* displaced by LS injection), and the total mass of tracer in all *previously* displaced pores associated with that cluster M_{old} (i.e. pores that were displaced by HS or LS at earlier times). Use these values to calculate a new average tracer concentration to assign to all pores within the cluster, $C_{clus} = (M_{old} + M_{new}) / V_{clus}$.

Appendix B: Salinity updates in flowing water-filled pores

For each global saturation change following the onset of LS injection, a designated period of convective tracer transport is simulated to determine the salinity evolution within the flowing bulk water. Assuming a source concentration of one (i.e. salinity = 0) at inlet pores, and using the previously calculated elemental flow values q, tracer concentrations C_{old} are updated as follows at each timestep Δt:

(i) calculate the mass of tracer flowing out of each bond, $M_{out} = q \cdot \Delta t \cdot C_{old}$;

(ii) sum the appropriate M_{out} values to determine the total mass of tracer M_{node} flowing into each node;

(iii) assuming perfect mixing in nodes, calculate the mass of tracer M_{in} entering each outflowing bond according to $M_{in} = q / q_{node} \cdot M_{node}$, where q_{node} represents the total flow into the node from all upstream bonds;

(iv) calculate the new tracer concentration C_{new} in each bond according to $C_{new} = C_{old} + (M_{in} - M_{out}) / V$, where V is the volume of the bond.

During the above procedure, the mass of tracer leaving any bond in a single timestep cannot be in excess of that available. Mass conservation therefore stipulates the condition $\Delta t = min\ (V / q)$, where the minimum is taken over all flowing bonds.

References

Agbalaka, C.C., Dandekar, A.Y., Patil, S.L., Khataniar, S., Hemsath J.R.: Coreflooding studies to evaluate the impact of salinity and wettability on oil recovery efficiency. Transport Porous Med. 76, 77-94 (2009)

Ashraf, A., Hadia, N.J., Torsæter, O., Tweheyo, M.T.: Laboratory investigation of low salinity waterflooding as secondary recovery process: effect of wettability. Paper SPE 129012 presented at the SPE Oil and Gas India Conference and Exhibition, Mumbai, 20 – 22 January (2010)

Austad, T., RezaeiDoust, A., Puntervold, T.: Chemical mechanism of low salinity water flooding in sandstone reservoirs. Paper SPE 129767 presented at the SPE Improved Oil Recovery Symposium, Tulsa, 24 – 28 April (2010)

Bernard, G.G.: Effect of floodwater salinity on recovery of oil from cores containing clays. Paper SPE 1725 presented at the 38th SPE California Regional Meeting, Los Angeles, 26 – 27 October (1967)

Blunt, M.J.: Effects of heterogeneity and wetting on relative permeability using pore level modelling. SPE J. 2, 70-87 (1997)

Blunt, M.J.: Flow in porous media – pore-network models and multiphase flow. Curr. Opin. Colloid In. 6, 197-207 (2001)

Buckley, J.S., Liu, Y., Xie, X., Morrow, N.R.: Asphaltenes and crude oil wetting – the effect of oil composition. SPE J. 2, 107-119 (1997)

Dixit, A.B., McDougall, S.R., Sorbie, K.S., Buckley, J.S.: Pore-scale modelling of wettability effects and their influence on oil recovery. SPE Reserv. Eval. Eng. 2, 25-36 (1999)

Fjelde, I., Asen, S.M., Omekeh, A.: Low salinity water flooding experiments and interpretation by simulations. Paper SPE 154142 presented at the 18th SPE Improved Oil Recovery Symposium, Tulsa, 14 – 18 April (2012)

Jadhunandan, P., Morrow, N.R.: Effect of wettability on waterflood recovery for crude-oil/brine/rock systems. SPE Reservoir Eng. 10, 40-46 (1995)

Lager, A., Webb, K.J., Black, C.J.J., Singleton, M., Sorbie, K.S.: Low salinity oil recovery – an experimental investigation. Paper presented at the International Symposium of the Society of Core Analysts, Trondheim, 12 – 16 September (2006)

Ligthelm, D.J., Gronsveld, J., Hofman, J.P., Brussee, N.J., Marcelis, F., van der Linde, H.A.: Novel waterflooding strategy by manipulation of injection brine composition. Paper SPE 119835 presented at the EUROPEC/EAGE Annual Conference and Exhibition, Amsterdam, 8 – 11 June (2009)

Martin, J.C.: The effects of clay on the displacement of heavy oil by water. Paper SPE 1411-G presented at the 3rd SPE Venezuelan Annual Meeting, Caracas, 14 – 16 October (1959)

Mahani, H., Berg, S., Ilic, D., Bartels, W.-B., Joekar-Niasar, V.: Kinetics of Low-Salinity-Flooding Effect. SPE J. 20, 8-20 (2015)

Mahmud, W.M., Arns, J.Y., Sheppard, A., Knackstedt, M.A., Pinczewski, W.V.: Effect of network topology on two-phase imbibition relative permeability. Transport Porous Med. 66, 481-493 (2007)

McDougall, S.R., Sorbie, K.S.: The application of network modelling techniques to multiphase flow in porous media. Petrol. Geosci. 3, 161-169 (1997)

McGuire, P.L., Chatham, J.R., Paskvan, F.K., Sommer, D.M., Carini, F.H.: Low salinity oil recovery: an exciting new EOR opportunity for Alaska's North Slope. Paper SPE 93903 presented at the SPE Western Regional Meeting, Irvine, 30 March – 1 April (2005)

Morrow, N.R., Tang, G-Q., Valat, M., Xie, X.: Prospects of improved oil recovery related to wettability and brine composition. J. Pet. Sci. Eng. 20, 267-276 (1998)

Morrow, N., Buckley, J.: Improved oil recovery by low-salinity waterflooding. J. Petrol Technol. 63, 106-112 (2011)

Patil, S., Dandekar, A.Y., Patil, S.L., Khataniar, S.: Low salinity brine injection for EOR on Alaska North Slope (ANS). Paper IPTC 12004 presented at the International Petroleum Technology Conference, Kuala Lumpur, 3 – 5 December (2008)

Sandengen, K., Tweheyo, M.T., Raphaug, M., Kjølhamar, A., Crescente, C., Kippe, V.: Experimental evidence of low salinity water flooding yielding a more oil-wet behaviour. Paper SCA2011-16 presented at the International Symposium of the Society of Core Analysts, Austin, 18 – 21 September (2011)

Shaker Shiran, B., Skauge, A.: Enhanced oil recovery (EOR) by combined low salinity water/polymer flooding. Energ. Fuel. 27, 1223-1235 (2013)

Shehata, A.M., Nasr-El-Din, H.A.: Role of sandstone mineral compositions and rock quality on the performance of low-salinity waterflooding. Paper IPTC 18176 presented at the International Petroleum Technology Conference, Kuala Lumpur, 10 – 12 December (2014)

Skauge A.: Low salinity flooding – a critical review. Paper presented at the 17th European Symposium on Improved Oil Recovery, St. Petersburg, 16 – 18 April (2013)

Sorbie, K.S., Collins, I.R.: A proposed pore-scale mechanism for how low salinity waterflooding works. Paper SPE 129833 presented at the SPE Improved Oil Recovery Symposium, Tulsa, 24 – 28 April (2010)

Tang, G.Q., Morrow, N.R.: Salinity, temperature, oil composition and oil recovery by waterflooding. SPE Reservoir Eng. 12, 269-276 (1997)

Tang, G.-Q., Morrow, N.R.: Influence of brine composition and fines migration on crude oil/brine/rock interactions and oil recovery. J. Pet. Sci. Eng. 24, 99 – 111 (1999a)

Tang, G.-Q., Morrow, N.R.: Oil recovery by waterflooding and imbibition – invading brine cation valency and salinity. Paper SCA-9911 presented at the International Symposium of the Society of Core Analysts, Golden, 1 – 4 August (1999b)

Yildiz, H.O., Morrow, N.R.: Effect of brine composition on recovery of Moutray crude oil by waterflooding. J. Pet. Sci. Eng. 14, 159 – 168 (1996)

Yousef, A., Al-Saleh, S., Al-Kaabi, A., Al-Jawfi, M.: Laboratory investigation of novel oil recovery method for carbonate reservoirs. Paper SPE 137634 presented at the Canadian Unconventional Resources and International Petroleum Conference, Calgary, 19 – 21 October (2010)